Journal of ELECTRONIC MATERIALS, Vol. 42, No. 7, 2013
DOI: 10.1007/s11664-012-2316-y

A Comparison Between the Mechanical and Thermoelectric Properties of Three Highly Efficient *p*-Type GeTe-Rich Compositions: TAGS-80, TAGS-85, and 3% Bi_2Te_3-Doped $Ge_{0.87}Pb_{0.13}Te$

JOSEPH DAVIDOW[1,2] and YANIV GELBSTEIN[1]

1.—The Department of Materials Engineering, Ben-Gurion University of the Negev, Beer-Sheva, Israel. 2.—e-mail: joseph.davidow@gmail.com

Since the 1960s, the TAGS system, namely $(GeTe)_x(AgSbTe_2)_{1-x}$, with two specific compositions $x = 0.8$ and 0.85, known as TAGS-80 and TAGS-85, respectively, was identified as containing highly efficient *p*-type thermoelectric materials. Recently, another highly efficient *p*-type GeTe-rich composition, namely 3% Bi_2Te_3-doped $Ge_{0.87}Pb_{0.13}Te$, achieving thermoelectric properties comparable to TAGS-based solid solutions, was also reported. Since all of these compositions were obtained by different manufacturing approaches, a comparison between the transport and mechanical properties of these alloys, prepared by the same manufacturing techniques, is required to identify the advantages and disadvantages of these compositions for practical thermoelectric applications. In the current research, the thermoelectric and mechanical properties of three highly efficient GeTe-rich alloys, TAGS-80, TAGS-85, and 3% Bi_2Te_3-doped $Ge_{0.87}Pb_{0.13}Te$, following hot pressing, were investigated and compared. Maximal ZT values of ~1.75, ~1.4, and ~1.6 at 500°C were found for these compositions, respectively. Improvement of the mechanical properties was observed by increasing the GeTe content. The influence of the GeTe relative amount on the transport and mechanical properties was interpreted by means of the phase-transition temperatures from the low-temperature rhombohedral to the high-temperature cubic phases.

Key words: TAGS, thermoelectrics, phase transition, lead germanium telluride, efficiency, figure of merit

INTRODUCTION

The development of practical thermoelectric devices for energy conversion from heat to electricity offers a major potential for overcoming the global energy crisis and atmospheric pollution, usually associated with fossil fuels. In addition, thermoelectric converters, without the involvement of any moving parts, are considered as suitable for long-term operation with minimal maintenance involvement. For this reason, such devices have been successfully used in deep-space missions, with minimal properties degradation, over several decades. The main disadvantage of such devices is their low thermal to electrical conversion efficiency. This has been the main motivation, during the last few years, for the development of highly efficient thermoelectric materials, capable of enhancement of the relevant efficiency, Ψ_{opt}, at least theoretically up to ~15% (Eq. 1), under normal operating conditions.

$$\Psi_{opt} = \frac{\Delta T}{T_H} \frac{\left(\sqrt{1+Z\overline{T}}-1\right)}{\sqrt{1+Z\overline{T}}+\frac{T_C}{T_H}}, \quad (1)$$

(Received July 6, 2012; accepted October 1, 2012; published online November 16, 2012)

where T_C and T_H are the cold- and hot-side temperatures, respectively, ΔT ($=T_H - T_C$) is the temperature difference along the device, and ZT is known as the thermoelectric figure of merit, defined in Eq. 2.

$$ZT = \frac{\alpha^2}{\kappa \cdot \rho} \cdot T, \tag{2}$$

where α is the Seebeck coefficient, κ is the thermal conductivity, and ρ is the electrical resistivity of the material.

It is obvious from Eq. 1 that Ψ_{opt} is proportional to ZT; therefore, maximization of α and minimization of κ and ρ of the involved thermoelectric materials will result in an enhancement of Ψ_{opt} for any given temperature difference. These three parameters, α, ρ, and κ, are all related such that an increase in electrical conductivity will lead to an increase in thermal conductivity. Again, Eq. 1 shows why this is so important when trying to improve the figure of merit.

Developments in new materials have been able to increase ZT by decreasing the thermal conductivity while leaving the electrical conductivity unchanged.

The thermal conductivity, κ, is composed of two contributions, from the lattice vibrations known as phonons and from charge carriers: κ_{ph} and κ_e, respectively, as presented in Eq. 3. The relationship between κ_e and the electrical conductivity, $\sigma = \rho^{-1}$, known as the Wiedemann–Franz law,[1] is also shown in this equation.

$$\begin{aligned} \kappa_{tot} &= \kappa_{ph} + \kappa_e \\ \kappa_e &= L\sigma T. \end{aligned} \tag{3}$$

One of the proposed methods of decreasing the thermal conductivity while leaving the electronic transport properties unchanged is by developing a method which will obstruct phonons. One such method to obstruct phonons has been suggested to be manipulation of the microstructure by introducing precipitates or submicron features into the matrix. This can be done by different alloying methods or by using phase-separation techniques such as spinodal decomposition, which leaves a fine and homogeneous microstructure dispersed with precipitates.[2]

Although highly efficient thermoelectric materials have recently been developed and reported, no practical thermoelectric converters with enhanced efficiencies have been reported to date. One possible reason is the insufficient mechanical properties usually apparent in most heavily doped semiconductors considered optimal for such applications. For this reason, enhanced thermoelectric properties are not the only criteria for enhanced thermoelectric devices, but rather a combination of enhanced thermoelectric and mechanical properties is required.

Group IV–VI-based compounds (e.g., PbTe, SnTe, and GeTe) and their solid solutions have been considered for many years as highly efficient thermoelectric materials for operating temperatures up to 500°C.[3] The most widely investigated compounds to date are PbTe-rich alloys, exhibiting high ZT values as both n-type (upon PbI_2 or Bi doping) and p-type (upon Na doping) elements. However, the mechanical properties of p-type Na-doped PbTe were found to be inferior to those of the n-type materials, and unsuitable for the demands of practical applications.[4]

The main factor limiting application of the Na-doped material is its pure elastic nature and the absence of even minor plasticity, preventing any plastic deformation that might occur during shaping and integration of the elements, when producing converters, or in normal operating conditions. GeTe-based compounds are considered as suitable p-type alternatives to PbTe, from a thermoelectric point of view. Solid solutions of GeTe and $AgSbTe_2$ form pseudobinary p-type semiconductors,[5] $(GeTe)_x(AgSbTe_2)_{1-x}$, commonly known by the acronym TAGS. In this system, two specific compositions with x values of 0.8 and 0.85, known as TAGS-80 and TAGS-85, respectively, have been reported as having optimal properties for thermoelectric applications and have been used in several deep-space missions.[6,7] Furthermore, it was reported that TAGS-80 has the potential to exhibit a higher maximal ZT value of ~1.7 compared with TAGS-85 ($ZT_{max} \approx 1.4$), both measured at 477°C, although the latter exhibits greater mechanical stability.[7] Recently, optimally doped solid solutions of GeTe and PbTe, in the form of $Ge_xPb_{1-x}Te$, have also shown very high thermoelectric potential with maximal ZT of ~1.8 at ~477°C for $x = 0.87$ and 3 mol.% Bi_2Te_3 doping.[8]

Although GeTe-based compounds exhibit very promising thermoelectric properties, an inherent instability of these materials is associated with the phase transition that these materials undergo from the low-temperature rhombohedral ($R3m$) structure to the high-temperature cubic ($Fm3m$) structure when being heated or cooled. For pure GeTe, the phase-transition temperature is 427°C,[8] an intermediate temperature between the hot- and cold-side temperatures of such thermoelectric converters under normal operating conditions. For this reason, it has been considered for many years that the intermediate location along the thermoelectric leg subjected to this phase-transition temperature has potential mechanical weaknesses originating from the high strain levels required to maintain coherence between the lattice planes of the two phases.

It has recently been observed using hot-stage x-ray diffraction (XRD) and differential scanning calorimetry (DSC) that the phase transition of GeTe-based compounds is of second order and therefore involves continuous variation of the lattice parameters of the two phases.[9] This is in contrast to the more common first-order phase

transition, in which a sharp variation of the lattice parameter at the phase-transition temperature is observed. Only in the latter case can mechanical instability at the transition temperature be expected, suggesting higher mechanical stability for GeTe-based compounds than was originally surmised.

In the current research, transport, structural, and mechanical properties of hot-pressed TAGS-80, TAGS-85, and 3 mol.% Bi_2Te_3-doped $Ge_{0.87}Pb_{0.13}Te$ solid solutions were analyzed and compared in an attempt to identify whether our recently developed Bi_2Te_3-doped $Ge_{0.87}Pb_{0.13}Te$ has the required advantages for incorporation into practical thermoelectric devices compared with the already proven potential of the TAGS system, prepared by the same methods.

EXPERIMENTAL PROCEDURES

Calculated amounts for TAGS-80, TAGS-85, and 3 mol.% Bi_2Te_3-doped $Ge_{0.87}Pb_{0.13}Te$ were mixed and sealed in an evacuated quartz ampoule under vacuum of 10^{-5} Torr. The ampoules were placed in a rocking furnace for 1 h at 800°C, then water quenched. The ingots were retrieved, then pulverized using a mortar and pestle, and sifted using a 60-mesh sieve to achieve particle size of 250 microns.

Subsequently, the samples were consolidated and sintered using an FCT HPW5 hot press. 3 mol.% Bi_2Te_3-doped $Ge_{0.87}Pb_{0.13}Te$ was hot-pressed for 60 min at 22 MPa and 450°C, and the TAGS-x samples were both hot-pressed for 30 min at 28.3 MPa and 450°C. These hot-pressing conditions were optimized to obtain nearly full (>96%) density, as presented in Table I.

Seebeck coefficient and electrical resistivity values were measured on rectangular samples (12 mm × 5 mm × 5 mm) using a Linseis LSR 3 system. The measurement was done in argon atmosphere of 1.2 bar up to 500°C. Thermal diffusivity and specific heat values were measured on disk-shaped samples (Ø ~12 mm × ~2.5 mm) using an LFA 457 Netzsch system. The thermal conductivity values were calculated as the product of the measured density, specific heat, and density (Table I).

The phase-transition temperature was measured by using both differential scanning calorimetry (DSC, STA 449; Netzsch) and hot-stage XRD. The samples for DSC were measured in powder form under argon atmosphere from room temperature to 500°C at 5 K/min.

Mechanical testing, consisting of compressive stress, microhardness, and Young's modulus testing, was performed on samples with the same dimensions as for Seebeck coefficient analysis. Microhardness testing was performed, using a Diamond-Head indenter, on a Vickers hardness scale with force of 980 mN for 10 s. The Young's modulus was measured using an ultrasonic method using the density values in Table I on a Panametrics Pulser Receiver device based on the pulse-echo method. To obtain adequate measurement statistics, microhardness as well as compression tests were carried out on three individual samples of each of the investigated compositions.

Compressive testing was performed on the hot-pressed samples using a universal testing machine (model 1445; Zwick). The length of the sample was measured before starting the test, and the machine evaluated the absolute change in length until failure occurred at a compression rate of 0.83 [1/s]. The values are summarized in Table II.

Table 1. Physical properties of the investigated samples

Sample	ρ $\left[\frac{g}{cm^3}\right]$	ρ_{Rel} [%]	C_p $\left[\frac{J}{gK}\right]$ (at 723 K)	α_{diff} $\left[\frac{mm^2}{s}\right]$
TAGS-80	6.15 ± 0.2	96.02	0.248	0.8720
TAGS-85	6.06 ± 0.2	98.47	0.265	0.9715
$Ge_{0.87}Pb_{0.13}Te$ + 3% Bi_2Te_3	6.37 ± 0.2	98.78	0.252	0.8505

ρ density, ρ_{Rel} relative density compared with the theoretical value in percent, C_p specific heat, α_{diff} thermal diffusivity.

Table 2. Mechanical properties of the investigated samples: E, elastic modulus; σ_{fail}, compressive failure stress; ε_{fail}, failure strain; HV, Vickers hardness value

Sample	E [GPa]	σ_{fail} [MPa]	ε_{fail} [%]	HV
TAGS-80	40.2 ± 0.4	50 ± 5	0.30 ± 0.05	181 ± 1
TAGS-85	42.7 ± 0.4	88 ± 8	0.31 ± 0.05	174 ± 1
$Ge_{0.87}Pb_{0.13}Te$ + 3% Bi_2Te_3	56.1 ± 0.5	112 ± 11	0.54 ± 0.07	179 ± 1

RESULTS AND DISCUSSION

Structural Properties

Phase-Transition Analysis

The phase-transition temperatures obtained by DSC, for the investigated compositions, from the low-temperature rhombohedral to the high-temperature cubic structures are shown in Fig. 1. The literature value for pure GeTe compound[4] is also shown. It can be seen that, by increasing the mole fractions of both of the NaCl cubic phases, i.e., $AgSbTe_2$ and PbTe, the phase-transition temperatures are decreased compared with the value (427°C) for the pure GeTe compound. This trend was expected since pure PbTe and $AgSbTe_2$ are uniphase throughout the entire examined temperature range. The transition temperatures of the investigated TAGS compositions were found in the range of 175°C to 240°C, while for Bi_2Te_3-doped $Ge_{0.87}Pb_{0.13}Te$ the transition temperature is higher (~373°C). These results indicate that, regardless of the nature of the phase transition (first or second order), avoiding the transition temperature, for example, by segmenting the investigated compositions with a low-temperature thermoelectric segment such as Bi_2Te_3, is possible only for the TAGS samples. This is due to the fact that Bi_2Te_3-based alloys are limited in their operation to ~300°C. Therefore, only materials exhibiting phase-transition temperatures lower than 300°C (i.e., the investigated TAGS samples) can be segmented with Bi_2Te_3 to avoid this transition completely. In the case of Bi_2Te_3-doped $Ge_{0.87}Pb_{0.13}Te$, the higher transition temperature of ~373°C will still be apparent even in the case of Bi_2Te_3 segmentation. This is clearly an advantage of the TAGS system.

To identify the nature of the phase transition, one characteristic composition, TAGS-85, was analyzed by hot-stage XRD in the temperature range from 30°C to 300°C, as shown in Fig. 2. In this figure, the low-temperature doublets, which are characteristic of the rhombohedral phase, and the high-temperature single peak patterns, indicating the high-temperature cubic phase, can easily be seen. In addition, it can be seen that the phase-transition temperature from the rhombohedral to the cubic phases is in the range from 100°C to 250°C, in agreement with the DSC results shown in Fig. 1. Nevertheless, the most important trend observed in this figure is the continuous variation of the lattice parameters (or the location of the rhombohedral doublets) to the high-temperature single-peak cubic phase. This observation clearly indicates the second-order nature of the phase transition, in contrast to the single-temperature phase transition associated with the more common first-order phase transition, which has also been corroborated by Cook et al.[9] Furthermore, this observation supports our initial assumption that, even in the vicinity of the phase transition, GeTe-rich materials are not susceptible to mechanical instability due to the fact that the lattice parameters of the two involved phases undergo a continuous change over a wide temperature range from one structure to the other rather than sharply at a single temperature. Only, in the latter case can high strain concentration be expected at a single location along the sample. The origin of the second-order phase transition in GeTe-based compounds can be better understood from Fig. 3. In this figure, the rhombohedral angle of the unit cell is plotted against the GeTe mole fraction for the various investigated compositions, as obtained from room-temperature XRD analysis. The low-temperature rhombohedral unit cell is very similar to the high-temperature cubic unit cell, exhibiting identical lattice parameters in all of the coordinates. The only difference between these structures is the angle between these parameters, called the rhombohedral angle. The high-temperature face-centered cubic phase angle is

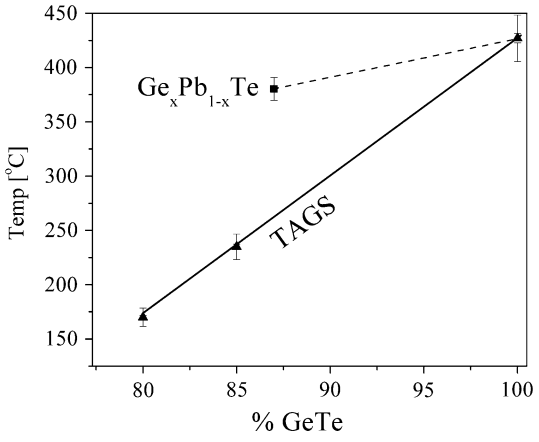

Fig. 1. Phase-transition temperatures of the investigated alloys depending on the GeTe mol.%, as evaluated by DSC.

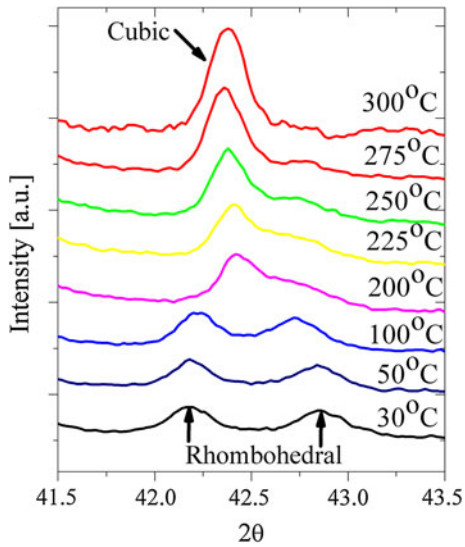

Fig. 2. Hot-stage XRD of TAGS-85.

obviously equal to 90°; however, it can be seen in the figure that, for the pure GeTe compound, the angle for the low-temperature rhombohedral phase is ~88.3°, a value which is quite similar to the 90° value for the high-temperature cubic phase. The high similarity between the low- and high-temperatures angles can be associated with the possibility of the lattice planes maintaining coherence, as observed in a second-order phase transition. In addition, it can be seen from the figure that Vegard's law is maintained for both the investigated $(GeTe)_x(PbTe)_{1-x}$ and $(GeTe)_x(AgSbTe_2)_{1-x}$ systems. This is in accordance with previous work performed on TAGS compounds, which showed that the rhombohedral angle corresponds to Vegard's law for an even broader range of TAGS-x compositions.[9]

As an intermediate summary, based on the DSC and XRD analyses, it can be stated that, when comparing TAGS and 3% Bi_2Te_3-doped $Ge_{0.87}Pb_{0.13}Te$, the advantage is in favor of TAGS, due to the ability for segmentation with Bi_2Te_3-based alloys which have exhibited higher efficiencies up to 300°C.[10] However, due to the second-order phase transition, $Ge_{0.87}Pb_{0.13}Te$ + 3% Bi_2Te_3 will still be able to withstand the phase transformation and not undergo mechanical failure due to lattice strain.

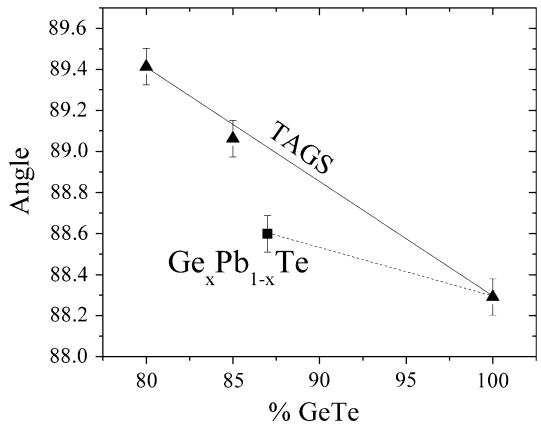

Fig. 3. Rhombohedral angle dependence on the GeTe mole fraction of the investigated alloys, as obtained by room-temperature XRD.

Microstructure Analysis

SEM imaging of the as-hot-pressed samples revealed that the microstructures of TAGS-80 and TAGS-85 were fairly homogeneous with a few dispersed precipitates, less than 5 μm in size, as seen in Fig. 4a, b. EDX analysis of TAGS-80 revealed that the precipitates are rich in silver and tellurium and poor in antimony. EDX of TAGS-85 showed that the microstructure is composed of three phases: a matrix with the nominal composition (taking into account the error of the EDX signal; Table III) of TAGS-85, and two secondary, germanium- and silver-rich phases. The Ge- or Ag-rich phases (or Te/Sb-diluted phases) can be attributed to the high vapor pressures of Te and Sb, which are the most volatile elements in the system. In contrast to the nearly homogeneous microstructure of the TAGS samples, the Bi_2Te_3-doped $Ge_{0.87}Pb_{0.13}Te$ consists of dispersed PbTe-rich phases located both at the grain boundaries and in a lamellar form, in which the white areas are rich in PbTe and the darker areas are rich in GeTe (Fig. 4c).

This latter effect can be attributed to phase separation of the matrix into PbTe- and GeTe-rich phases, due to the miscibility gap apparent between these phases.[11]

Mechanical Properties

The mechanical properties of the three investigated compositions, namely the Young's modulus, E, compressive failure strength, σ_{fail}, compressive failure strain, ε_{fail}, and the Vickers microhardness, HV, are listed in Table II. Since GeTe alloys are known for their brittle characteristics, ultrasonic resonant testing can be used to identify the elastic moduli and for nondestructive preliminary analysis of the samples. The Young's moduli of the samples were calculated according to Eq. 4 using the measured values of density and lateral/transverse

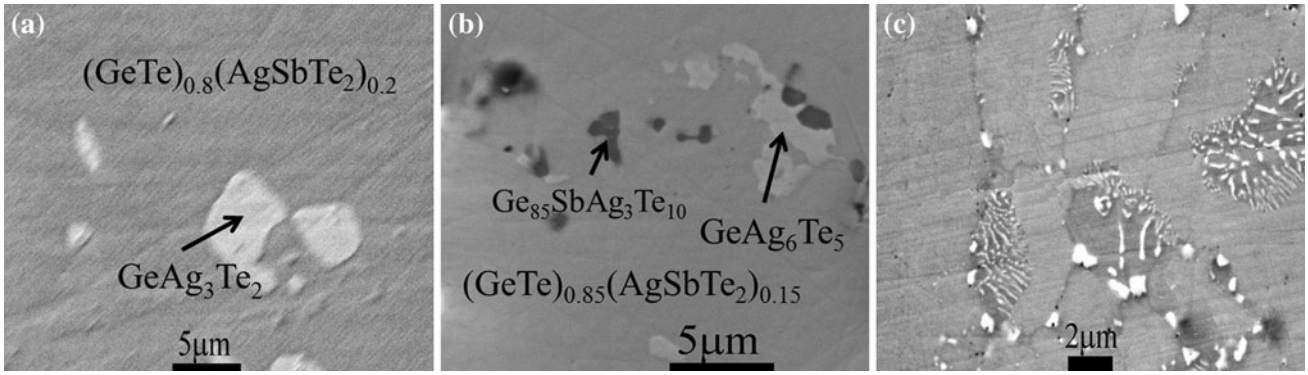

Fig. 4. SEM backscattered electron (BSE) micrographs of (a) TAGS-80, (b) TAGS-85, and (c) $Ge_{0.87}Pb_{0.13}Te$ + 3% Bi_2Te_3, following hot pressing.

Table 3. Compositions in atomic percent of the evaluated samples

	Element	Ge	Sb	Ag	Te	Pb	Bi
TAGS-80	Theoretical	33.33	8.33	8.33	50	0	0
	EDS	33.65 ± 2	8.27 ± 0.8	8.29 ± 0.6	49.79 ± 1	0	0
TAGS-85	Theoretical	36.96	6.52	6.52	50	0	0
	EDS	36.25 ± 2	6.33 ± 0.8	6.2 ± 0.6	51.22 ± 1	0	0
$Ge_{0.87}Pb_{0.13}Te$	Theoretical	42.178	0	0	50.315	6.307	1.2
	EDS	39.6178 ± 2	0	0	52.508.6 ± 3	6.506 ± 0.4	1.3682 ± 0.8

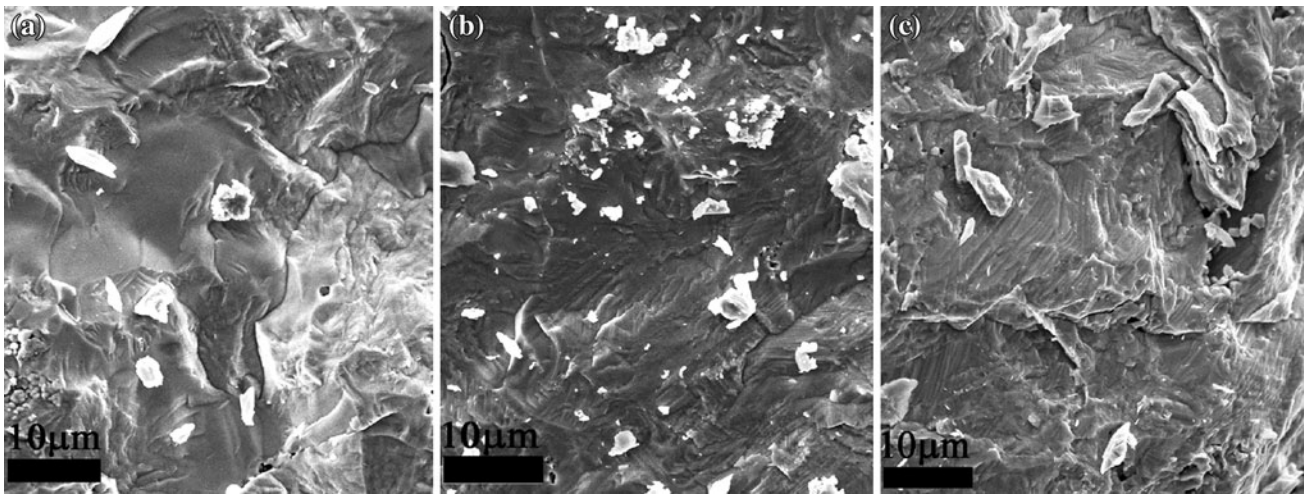

Fig. 5. Fractography images of: (a) TAGS-80, (b) TAGS-85, and (c) $Ge_{0.87}Pb_{0.13}Te$ + 3% Bi_2Te_3, following mechanical compression testing.

speeds of sound (measured by ultrasonic resonant testing).

$$E = 3\rho C_t \cdot \frac{C_l^2 - \frac{4}{3}C_s^2}{C_l^2 - C_s^2}, \quad (4)$$

where ρ is the sample's density, and C_l and C_s are the lateral and transverse speeds of sound, respectively. On comparing the two investigated TAGS compositions, similar Young's modulus values were expected,[12] due to the similar chemical bonding in both compositions. The Young's modulus of $Ge_{0.87}Pb_{0.13}Te$ is higher than that of the TAGS system due to the introduction of Pb into the solid solution.

Fractography images were taken following compressive testing of three samples of each composition for statistical analysis (Fig. 5). The images show that all three compositions are of brittle nature, as indicated by the intragranular fracture. However, the images cannot provide additional information regarding which of the compositions is stronger or even which is more brittle. To answer these questions, compressive stress–strain values were deduced from the experiment and are summarized in Table II. Here, it can be clearly seen that TAGS-80 is more prone to failure and therefore inferior for practical usage in thermoelectric devices compared with TAGS-85, as previously postulated.[7]

Furthermore, it can be seen from Table II that, although the microhardness values obtained show similar values for all of the investigated samples, the $Ge_{0.87}Pb_{0.13}Te$ composition exhibited higher compressive failure stress and strain values, σ_{fail} and ε_{fail}, respectively, compared with the TAGS system. This indicates that higher possible maximal stresses under higher deformation levels of the former are required to maintain the integrity of the samples under operating conditions.

This result clearly indicates a clear advantage for the $Ge_{0.87}Pb_{0.13}Te$ composition, compared with TAGS, from the point of view of mechanical properties.

Transport Properties

The temperature dependencies of the Seebeck coefficient, electrical resistivity, thermal conductivity, and dimensionless figure of merit, *ZT*, of the investigated samples are shown in Figs. 6–8 and discussed in greater detail below.

For all the examined samples, an abnormal temperature dependence of all the electronic transport properties is observed as a slope change in the vicinity of the phase-transition temperature

(Fig. 1), resulting from the phase transition from the low-temperature rhombohedral to the high-temperature cubic phases. It can be seen in (Fig. 6a, b) that both α and ρ values decrease while moving from TAGS-80 via TAGS-85 to $Ge_{0.87}Pb_{0.13}Te$, for almost any given temperature. This evidence can be attributed to the increased concentration of GeTe, which is known to exhibit very high hole concentration and therefore very low Seebeck coefficient and electrical resistivity values. Hence, increasing the GeTe concentration of the investigated samples results in decrease of both α and ρ values. The effect of the lower carrier concentration of the TAGS samples compared with that of $Ge_{0.87}Pb_{0.13}Te$ can also be observed by the onset of intrinsic conduction at lower temperature, observed as a reduction in both α and ρ values at lower temperatures for the former. The same effect can also be observed by the opposite trends of the low-temperature thermal conductivity values (Fig. 7a) compared with those of α and ρ, indicated by a reduction in κ values with decreasing charge carrier density, or GeTe concentration, due to a more pronounced electronic effect on the thermal conductivity. However, at higher temperatures, where the influence of phonons is more pronounced, the lowest κ values are observed for the $Ge_{0.87}Pb_{0.13}Te$ sample, as can be explained by further investigation of the lattice thermal conductivity variations with temperature (Fig. 7b). These values were obtained by subtraction of the electronic contribution to the thermal conductivity, as calculated using the Wiedemann–Franz law (Eq. 3), from the total thermal conductivity values measured using the LFA device (Fig. 7a). It can be seen from this graph that, at lower temperatures, the 3% Bi_2Te_3-doped $Ge_{0.87}Pb_{0.13}Te$ sample shows a higher value than both of the TAGS compositions. This is due to the lattice thermal conductivity of the constituents of the solid solution of both the TAGS and of the $Ge_{0.87}Pb_{0.13}Te$ sample. The κ_l value of $AgSbTe_2$ is 0.7 $\frac{W}{mK}$, that of GeTe is 1.3 $\frac{W}{mK}$, and that of PbTe is 2.3 $\frac{W}{mK}$.[13] This is thought to be the reason why the

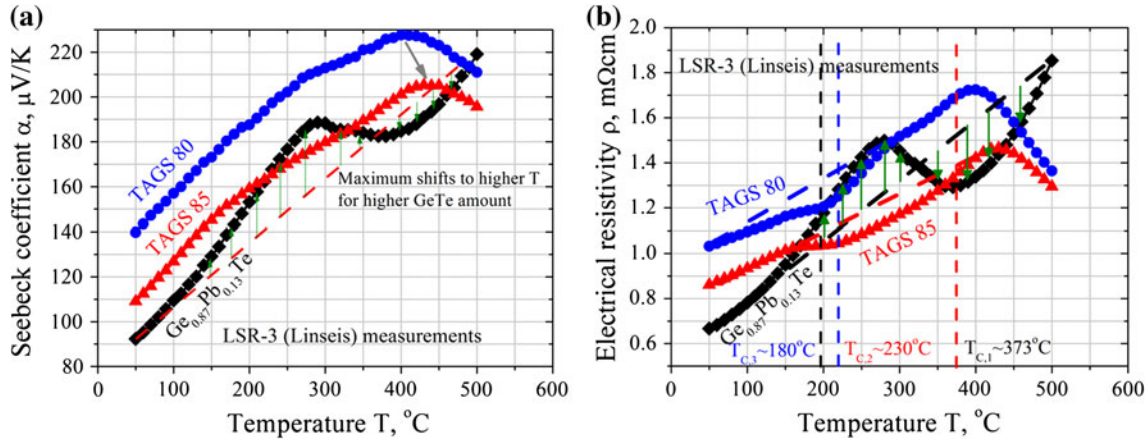

Fig. 6. Temperature dependence of: (a) Seebeck coefficient, and (b) electrical resistivity of the investigated samples.

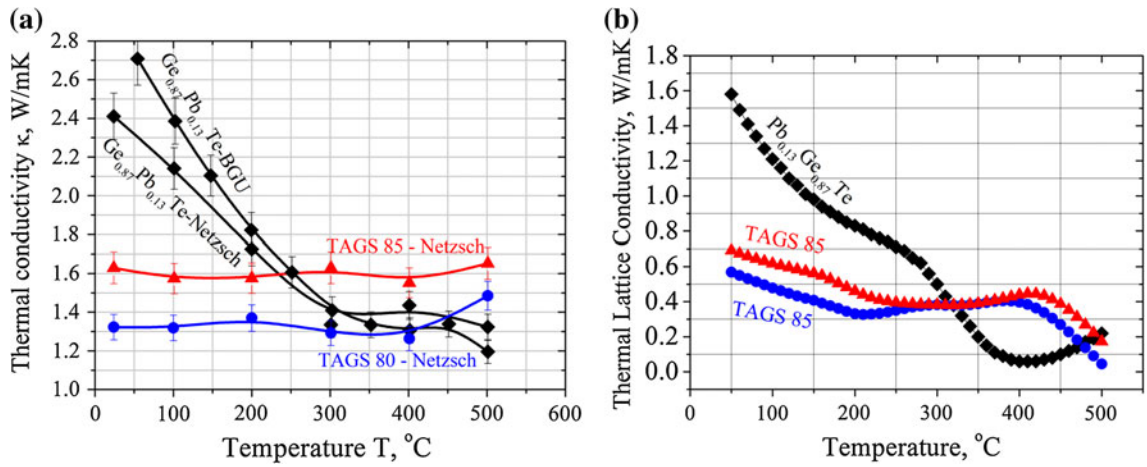

Fig. 7. Temperature dependence of (a) total thermal conductivity, and (b) lattice thermal conductivity of the investigated samples.

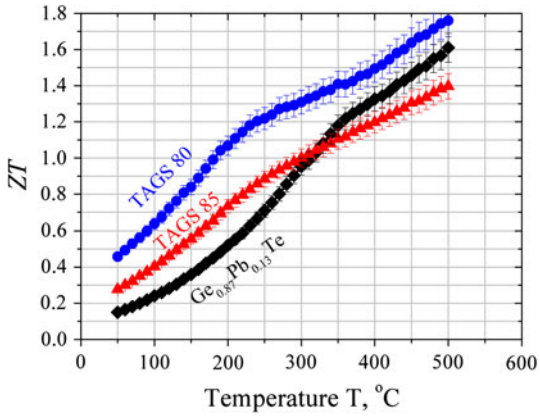

Fig. 8. Temperature dependence of the dimensionless figure of merit, *ZT*, of the investigated samples.

lattice thermal conductivity of $Ge_{0.87}Pb_{0.13}Te$ is much higher than that of both the TAGS compositions, since $Ge_{0.87}Pb_{0.13}Te$ consists of PbTe and GeTe, both of which have higher values than that of $AgSbTe_2$. However, a sharp decrease can be seen closer to the phase-transition temperature of all of the investigated samples. In the case of $Ge_{0.87}Pb_{0.13}Te$, due to the fact that the phase-transition temperature is higher compared with the TAGS samples, the κ_l values of this sample are lower than the other investigated compositions at around the same temperature where the electronic transport components are at their maximum. This is in contrast to the TAGS samples, where the transition occurs at a much lower temperature than is optimal from the thermoelectric point of view. The dimensionless figure of merit, *ZT*, of the investigated samples is shown in Fig. 8. It is apparent that the TAGS-85 sample is less optimal thermoelectrically than the TAGS-80 sample. In light of these *ZT* values of all three investigated compositions, it would seem more efficient to utilize TAGS-80 in thermoelectric devices. However, as stated above in the "Introduction," having a high figure of merit is not enough to warrant use of a certain material. Figure 8 shows that TAGS-80 has a higher *ZT* value than both TAGS-85 and $Ge_{0.87}Pb_{0.13}Te$, and yet both of these compositions exhibit better mechanical properties than TAGS-80. Possible segmentation of TAGS-85 for operating temperatures up to 320°C and 3% Bi_2Te_3-doped $Ge_{0.87}Pb_{0.13}Te$ at higher temperatures is the most promising optimization route. Otherwise, if the maximal operating temperature is 320°C, TAGS-85 is thermoelectrically favorable, and for higher temperatures, the 3% Bi_2Te_3-doped $Ge_{0.87}Pb_{0.13}Te$ composition is advantageous.

CONCLUSIONS

Three highly efficient *p*-type thermoelectric materials, namely two proven compositions of the known TAGS system and one recently developed $Pb_xGe_{1-x}Te$ composition, were tested extensively following similar sample preparation methods to identify their potential from both transport and mechanical properties points of view. From a thermoelectric point of view, TAGS-80 exhibited the highest *ZT* value of 1.75, followed by $Ge_{0.87}Pb_{0.13}Te$ + 3% Bi_2Te_3, which showed an impressive maximum *ZT* value of ~1.6. The latter results were mainly attributed to low thermal conductivity values, due to a phase-transition temperature close to that of the optimal electronic transport properties, consequently resulting in low lattice thermal conductivity and high maximal *ZT*. From the mechanical properties point of view, $Ge_{0.87}Pb_{0.13}Te$ + 3% Bi_2Te_3 shows a clear advantage at room temperature compared with the investigated TAGS compositions, exhibiting higher compressive failure stress and strain values. It was shown that, although $Ge_{0.87}Pb_{0.13}Te$ + 3% Bi_2Te_3 undergoes a phase transition at temperatures above 300°C, thus preventing use of segmentation by low-temperature Bi_2Te_3-based segments to avoid the phase transition, no high-temperature mechanical weakness is to be expected in the vicinity of the phase-transition temperature, due to the second-order nature of this transition.

In summary, it can be claimed that the $Ge_{0.87}Pb_{0.13}Te$ + 3% Bi_2Te_3 composition exhibits very high potential, from both mechanical and transport properties points of view, for utilization in practical thermoelectric applications. Furthermore, it was found to be comparable to the well-known TAGS samples which have continued to operate for several decades in deep-space thermoelectric missions.

REFERENCES

1. G. Chen, M.S. Dresselhaus, G. Dresselhaus, J.P. Fleurial, and T. Caillat, *Int. Mater. Rev.* 48, 45–66 (2003).
2. H.J. Goldsmid and A.W. Penn, *Phys. Lett. A* 27, 523–524 (1968).
3. L. Flanders, K.R. Cummer, J. Feinsinger, and B. Heshmatpour, *AIP Conf. Proc.* 813, 560 (2006).
4. Y. Gelbstein, G. Gotesman, Y. Lishzinker, Z. Dashevsky, and M.P. Dariel, *Scr. Mater.* 58, 251–254 (2008).
5. F.D. Rosi, J.P. Dismukes, and E.F. Hockings, *Electr. Eng.* 79, 450 (1960).
6. C. Wood, *Rep. Prog. Phys.* 51, 459–539 (1988).
7. E.A. Skrabek and D.S. Trimmer, *CRC Handbook of Thermoelectrics*, ed. D.M. Rowe (Boca Raton: CRC, 1995), p. 267.
8. Y. Gelbstein, B. Dado, Ohad Ben-Yehuda, Y. Sadia, Z. Dashevsky, and M.P. Dariel, *JEM*. (2009).
9. B.A. Cook, M.J. Kramer, X. Wei, J.L. Harringa, and E.M. Levin, *J. Appl. Phys.* 101, 053715 (2007).
10. V.L. Kuznetsov, L.A. Kuznetsova, A.E. Kaliazin, and D.M. Rowe, *J. Mater. Sci.* 37, 2893–2897 (2002).
11. Y. Gelbstein, B. Dado, O. Ben-Yehuda, Y. Sadia, Z. Dashevsky, and M.P. Dariel, *Chem. Mater.* 22, 1054–1058 (2010).
12. J.R. Salvador, J. Yang, X. Shi, H. Wang, and A.A. Wereszczak, *J. Solid State Chem.* 182, 2088–2095 (2009).
13. D.P. Spitzer, *J. Phys. Chem. Solids* 31, 19–40 (1970).